

RELATIONSHIPS BETWEEN SIZE, NUMBER AND DENSITY OF AXOSOMATIC BOUTONS AND MOTOR NEURONAL SIZE

MARK DeSANTIS

*Department of Biological Sciences and Washington, Alaska,
Montana, Idaho Medical Program
University of Idaho
Moscow, Idaho 83843, U.S.A.*

and

VISAKA LIMWONGSE

*School of Dentistry, Chulalongkorn University
Bangkok 10500, Thailand*

(Received May 12, 1983; in final form, August 4, 1983)

Abstract

Analysis of electron microscopic data revealed positive correlations between a motor neuron's diameter and the amount of axosomatic input it received. An increase in the number of boutons, more than an increase in their size, accounted for the greater amount of somal membrane covered by boutons on larger motor neurons. The number of boutons apposing a motor neuron's soma had a lower limit predicted by the surface area of its cell body; the upper limit was correlated with the somal volume. The increase in the number of boutons as a function of a motor neuron's size was large enough to result in a calculated density of axosomatic boutons that was directly related to the diameter of a motor neuron's soma. We have interpreted these relationships based on biological events that occur in neurons.

1. Introduction

Synapses on the cell body of a multipolar neuron are especially important since they potently influence the voltage difference across the neurolemma at the initial segment, where action potentials are initiated (Rall, 1967). Within a relatively homogeneous population of mammalian multipolar neurons, there is evidence that those with larger cell bodies have a greater percentage of the soma covered by boutons that make a synapse than do those with smaller cells bodies (Bowsher and Westman, 1971; Westman, 1971a, b; Westman and Bowsher, 1971; Kojima *et al.*, 1971; Nakamura, 1975; Limwongse and DeSantis, 1980). The existence of and basis for this relationship have scarcely been explored.

In this paper we use data about axosomatic boutons on mammalian motor neurons to show that: 1) the greater amount of the somal surface covered by boutons on large motor neurons relative to small ones is primarily due to a greater number rather than a greater size of boutons, 2) the direct relationship between the number of boutons and the size of the postsynaptic motor neuron is correlated at a lower limit with the surface area and at an upper limit with the volume of the motor neuron's soma, and 3) the increase in the number of boutons as a function of motor neuronal size is large enough to result in a calculated density of axosomatic boutons that is a direct, curvilinear function of motor neuronal diameter.

2. Methods

The data used here were from electron microscopic studies by Kojima *et al.* (1972) for 36 neurons within the motor nucleus of the cat's C6-7 spinal cord segments and by Limwongse (1980) for 68 trigeminal motor neurons in the rat's brain stem. These two studies provided a relatively large sample, a full range of cell body sizes, and similar types of measures for axosomatic boutons on motor neurons which innervate muscles that act across synovial joints and encounter a relatively wide range of variability in load. Scatter diagrams were constructed from values (i.e. percent of motor neuron's surface covered by boutons, mean arithmetic length of boutons, number of boutons, and diameter of the motor neuron) obtained from both sources. Each point on a scatter diagram represents data for the profile of one motor neuron. For 90 of the 104 neurons, the plane of the section from which measurements were made included the nucleus of the cell.

Programmable calculators (Hewlett-Packard 25C and 11C) were used to fit linear ($Y = a + bX$), logarithmic ($Y = a + b \ln X$), exponential ($Y = ae^{bX}$), and power ($Y = aX^b$) equations to the data points of each scatter diagram. The relationship between ordinate and abscissa values is given by the coefficient of determination (r^2) for these simple linear and curvilinear correlations (Sokal and Rohlf, 1969). The straight line and the best fitting line, which always happened to be curvilinear, are shown on scatter diagrams of Figures 1, 2, 3 and 8. Multiple linear and curvilinear correlations were done using a Statistical Analysis System (SAS) program on an IBM 4341 computer. For these multiple correlations, the relationship between parameters is given by the coefficient of multiple determination (R^2) (Sokal and Rohlf, 1969).

3. Results

Percentage of Soma Covered by Boutons

The scatter diagram in Figure 1 shows that the percentage of the perimeter of a motor neuron which was covered by axosomatic boutons (y) was directly related to the diameter of the motor neuron's cell body (ψ). The data points were fit ($r^2 = 0.73$, Table 1) by the linear equation

$$(1) \quad y = -19.14 + 2.34\psi$$

An even better fit to the data ($r^2 = 0.77$, Table 1) was obtained with the logarithmic equation

$$(2) \quad y = -179.09 + 69.08 \ln \psi$$

The positive correlation between y and ψ could have occurred because either there were larger boutons on larger neurons or more boutons on larger neurons or because both conditions applied.

Size of Axosomatic Boutons

Analyses of serial sections (Conradi, 1969) and freeze-fracture replicas (Voss *et al.*, 1980) show that boutons appose circular and elliptical areas at a motor neuron's

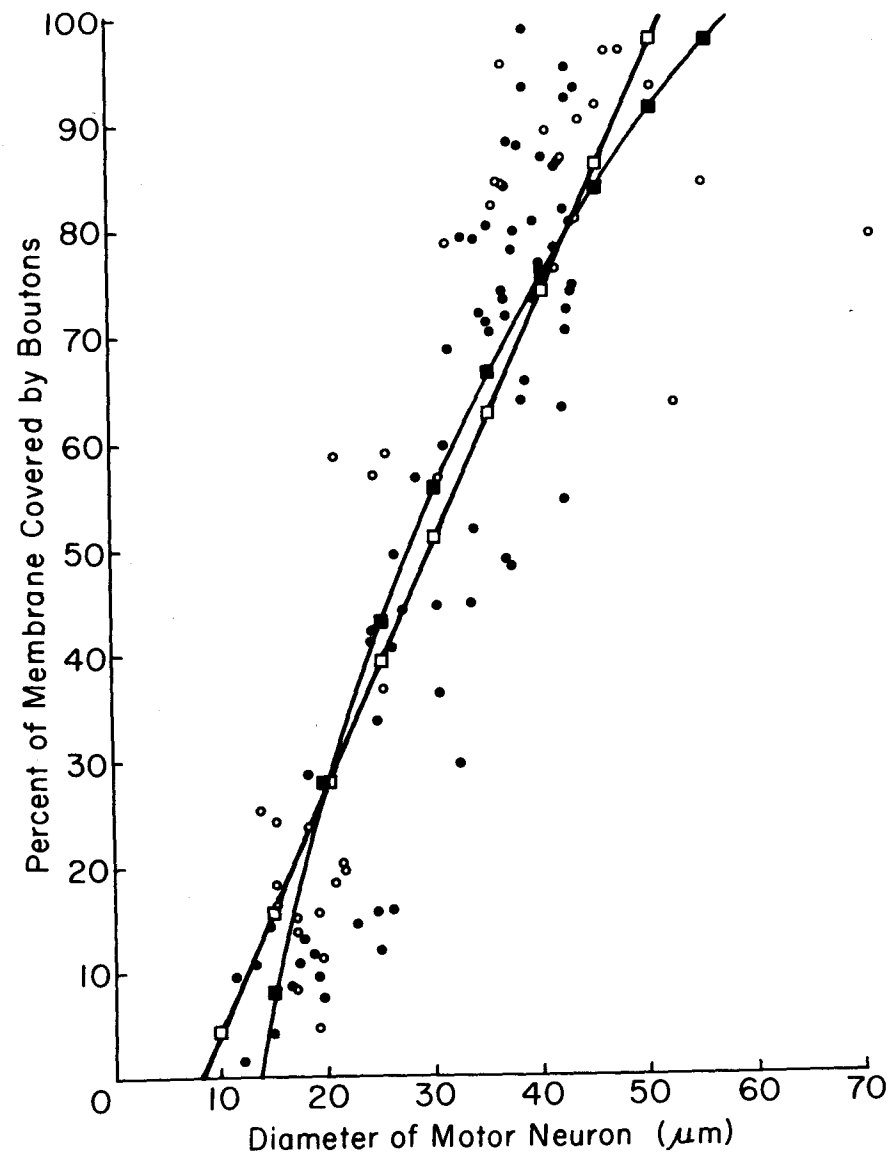


Fig. 1. Percent of somal membrane covered by boutons for neurons of different diameter. The data in this and subsequent scatter diagrams are from Kojima *et al.* 1972 (○) and Limwongse 1980 (●). A linear estimation (□, equation 1) and a logarithmic curve (■, equation 2) have been fit to the data.

surface, and the average length of a bouton's profile approximates its average diameter of apposition (Conradi, 1969). Figure 2 is a scatter diagram of the mean length for all axosomatic boutons (y') on each motor neuronal profile plotted against the motor neuron's somal diameter (ψ). There was a positive relationship. The linear equation that fit these data ($r^2=0.37$, Table 1) was

$$(3) \quad y' = 1.32 + 0.02\psi$$

The data points were fit slightly better ($r^2=0.40$, Table 1) by the power equation

$$(4) \quad y' = 0.69\psi^{0.29}$$

Although some degree of correlation may have been present, the average variation in the length of boutons was poorly predicted from the size of the motor neuronal soma to which they were apposed.

Number of Axosomatic Boutons

On the other hand, there was also a positive relation between the number of axosomatic boutons (y'') and the motor neuron's diameter (ψ), as is shown in Figure 3. The linear equation which fit these data ($r^2=0.73$, Table 1) was

$$(5) \quad y'' = -27.17 + 2.04\psi$$

This scatter diagram was fit much better ($r^2=0.83$, Table 1) by the power curve

$$(6) \quad y'' = 4.312 \times 10^{-3} \psi^{2.56}$$

This indicated that a relatively high degree of the variance in the number of boutons was accounted for by variation in the diameter of the motor neuron which they apposed. The direct relationship, then, between the percentage of coverage by axosomatic boutons and the diameter of a motor neuron (Figure 1) was due chiefly to a greater number of boutons, rather than to a larger size of boutons, on larger motor neurons.

Since the power function in equation (6) had an exponent of 2.56, it seemed that the increase in the number of axosomatic boutons as a function of motor neuronal size might be better accounted for by a cubic (volume) or square (surface area) increase in the size of a motor neuron's soma rather than by a linear (diameter) one. To explore this possibility, curves were constructed to predict what the increase in the number of boutons should be if it was a function of either the volume, surface area or diameter increase in motor neuronal size. The arithmetic mean values for the number of boutons, volume, surface area and diameter were calculated for those motor neurons less than 20 μm diameter. The mean number of boutons and the mean diameter for the motor neurons less than 20 μm diameter were calculated from the original data (Kojima *et al.*, 1972; Limwongse, 1980). As a simplifying assumption, the neuronal cell body was represented by a sphere, and standard equations were used to calculate volume (V)

$$(7) \quad V_1 = \frac{\pi d^3}{6}$$

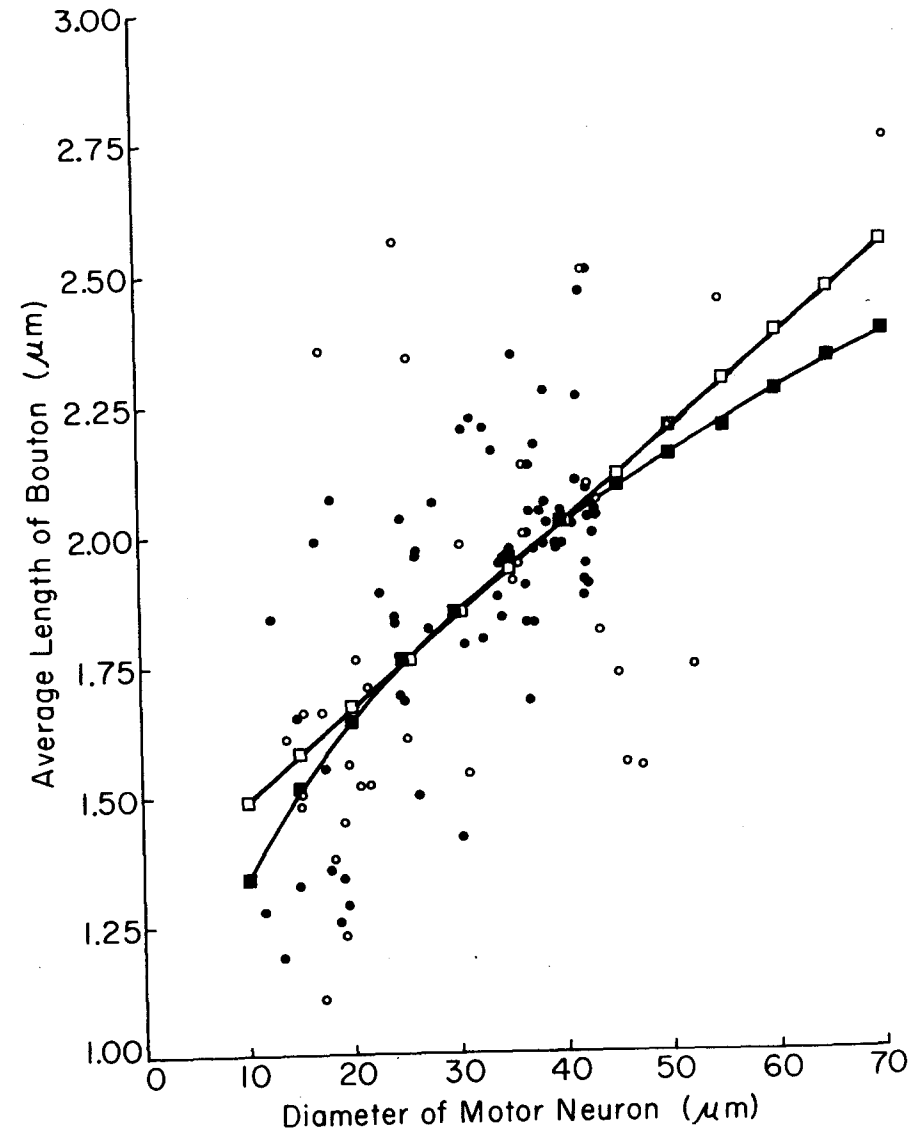


Fig. 2. Mean length of axosomatic boutons on motor neurons of different diameter. A linear estimation (\square , equation 3) and a power curve (\blacksquare , equation 4) have been fit to the data.

and surface area (SA)

$$(8) \quad SA_1 = \pi d^2$$

of a cell body, with d being the mean somal diameter. A reason for selecting the averages for the smallest motor neurons (i.e. those less than $20 \mu\text{m}$ diameter) as a starting point for making predictions was that all spinal motor neurons of the kitten are relatively small at birth, but some increase dramatically in size during the following two months (Sato *et al.*, 1977). Values for the predicted number of boutons were calculated by solving for \hat{y}'' in the ratio

$$(9) \quad \hat{y}'' = \frac{y''_{\text{small}} \cdot \psi'}{\psi''_{\text{small}}}$$

where ψ' was an arbitrarily selected size of a cell body (either a volume, surface area or diameter), y''_{small} was 5.48 (i.e. the average number of boutons calculated for those motor neurons less than $20 \mu\text{m}$), and ψ''_{small} was, respectively, the average volume ($2408.10 \mu\text{m}^3$), surface area ($868.83 \mu\text{m}^2$) or diameter ($16.63 \mu\text{m}$) calculated for those motor neurons less than $20 \mu\text{m}$. Figure 4 shows the predictions for the number of boutons expected on the basis of increases in a motor neuron's volume, surface area and diameter. The curves based on the former two measures straddle most of the data points, and the power curve shown in Figure 3. In an attempt to decide whether surface area or volume was the better predictor for the number of boutons, an estimate of \hat{y}'' was made for each of the neurons using equation (9) by substituting the ratio estimator for either surface area or volume and each motor neuron's diameter. Those values were compared separately to the corresponding value of y'' obtained using equation (6). The coefficient of determination for \hat{y}'' with y'' was slightly higher using the ratio estimator for volume ($r^2 = 0.99$) than with the one for surface area ($r^2 = 0.98$).

Another approach was available to judge whether the number of axosomatic boutons is better predicted by the surface area or the volume of the postsynaptic neuron. If the number of boutons is plotted as a function of the motor neuron's surface area and again as a function of the motor neuron's volume, the larger coefficient of determination (r^2) should identify which best accounts for variation in the number of axosomatic boutons. Unlike somal diameter, which was directly measured from a neuronal profile sectioned through its approximate center, the surface area and volume of a neuron had to be calculated from the linear measures. Several procedures were available to do that. To calculate somal surface area (SA), we used equation (8) and equation (10) (Ulfhake and Cullheim, 1981).

$$(10) \quad SA_2 = \pi d_1 d_2$$

To calculate somal volume (V), we used equation (7), equation (11) (Ulfhake and Cullheim, 1981) and equation (12) (Schadé and Van Harreveld, 1961).

$$(11) \quad V_2 = \frac{\pi d_1 d_2^2}{6}$$

$$(12) \quad V_3 = \frac{1.04 \pi d_1 d_2 \sqrt{d_1 d_2}}{6}$$

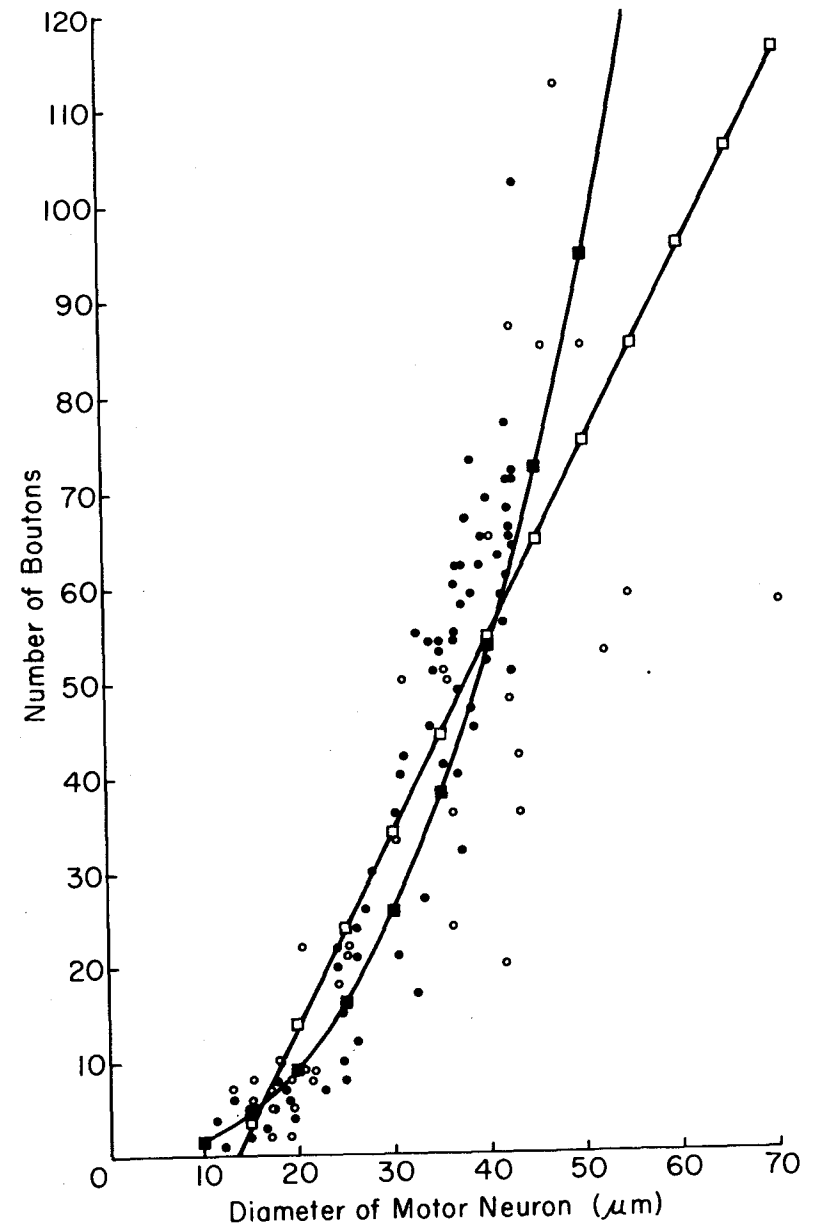


Fig. 3. Number of axosomatic boutons on neurons of different diameter. A linear estimation (□, equation 5) and a power curve (■, equation 6) have been fit to the data.

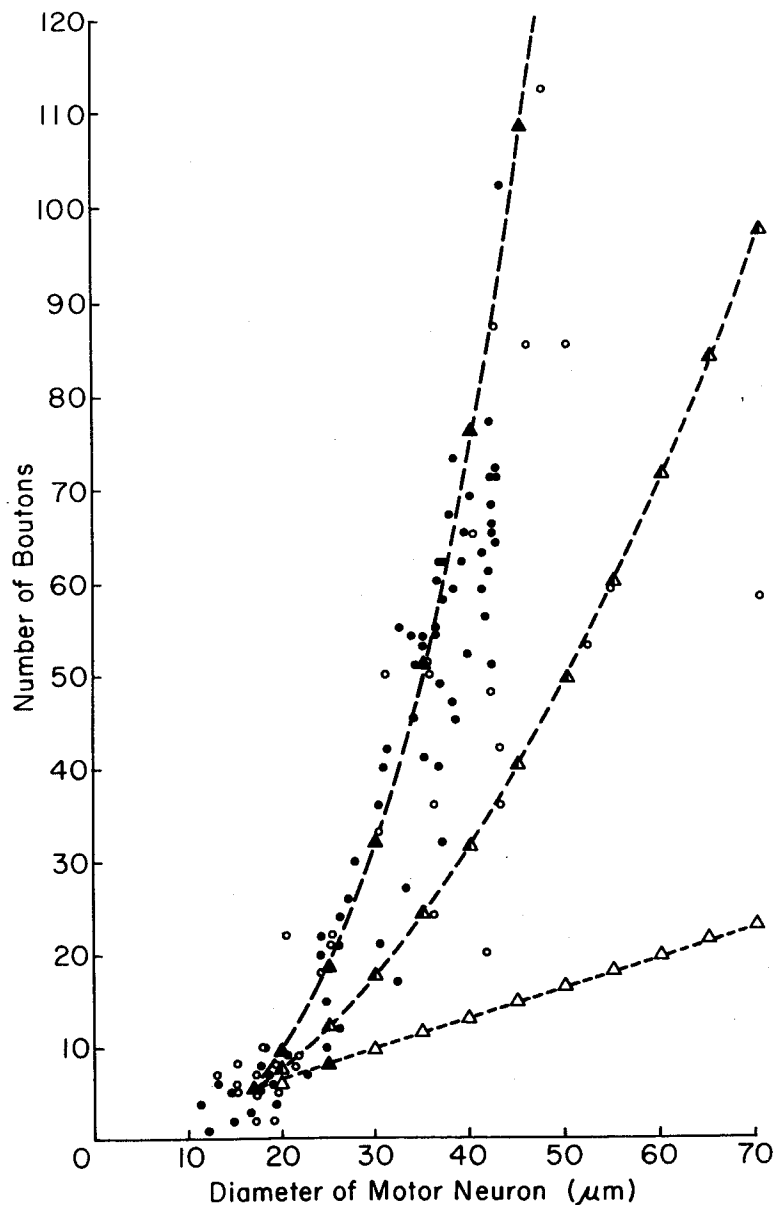


Fig. 4. The number of axosomatic boutons predicted to occur (equation 9) on neurons of different diameter as the volume (▲), surface area (△) and diameter (△) of the postsynaptic cell body were increased is shown relative to the scatter diagram, which is the same as in Figure 3.

Table 1
Coefficients of Determination (r^2) for Simple Linear and Curvilinear Correlations Between Various Parameters for Boutons and Diameter of Motor Neuron's Soma^a

Bouton Parameter	Type of Correlation			power
	linear	logarithmic	exponential	
Percent of Soma Perimeter Covered by Boutons	0.73	0.77*	0.66	0.74
Mean length of Boutons	0.37	0.38	0.37	0.40*
Number of Boutons	0.73	0.74	0.75	0.83*
Density of Boutons equation 18	0.55†	0.59†	0.61†	0.69*†
equation 19	0.46	0.51	0.48	0.55*
equation 22	0.47	0.53	0.48	0.56*

^a all coefficients of determination were highly significantly greater than zero ($P < .01$)
 * best correlation across row
 † best correlation down column for methods of determining density of boutons.

Table 2
Coefficients of Determination (r^2) for Simple Linear Correlations Between Number and Density of Boutons with Surface Area and Volume of a Motor Neuron's Soma^a

Bouton Parameter	Motor Neuronal Soma	
	Surface Area	Volume
Number	πd^2 0.62*	$\frac{\pi d^3}{6}$ 0.44
Density	$\pi d_1 d_2$ 0.39†	$\frac{\pi d_1 d_2^2}{6}$ 0.32
equation 18	0.42*†	0.26†
equation 19	0.35	0.21
equation 22	0.35*	0.20
		$\frac{1.4\pi d_1 d_2 \sqrt{d_1 d_2}}{6}$ 0.39
		0.22
		0.23†
		0.19

^a all coefficients of determination were highly significantly greater than zero ($P < .01$)
 * best linear correlation across row
 † best linear correlation down column for methods of determining density of boutons.

Equations (10), (11) and (12) allow for using major (d_1) and minor (d_2) axes of the cell body rather than assuming either a constant or an average diameter. Table 2 gives the coefficients of determination (r^2) for correlations between the number of boutons and calculated values of either somal surface area or volume. In this case, variation in the number of boutons was better accounted for by the surface area than by the volume of the motor neuron's soma, as denoted by the larger values of r^2 (Table 2). The linear regressions giving the best fits to the scatter diagrams for number of boutons with surface area (Figure 5A) and volume (Figure 5B) are shown on semilogarithmic plots, which is why the lines that fit them best appear curved. Plotting the data this way allowed for comparison of the relative slopes of the linear regressions at similar places along the abscissa, and the relative goodness of fit to the data points is shown more clearly and efficiently than using linear scales for both axes.

Using Size and Number of Boutons to Account for the Percent of the Surface Covered by Boutons on Motor Neurons of Different Diameter

If the parameters of size (y') and number (y'') of boutons are sufficient to account for the percentage of a motor neuron's surface that is covered by boutons (y), then it should be possible to predict accurately the latter value (\hat{y}) from the product of the former two features multiplied by a factor to convert to percent.

$$(13) \quad \hat{y} = (y')(y'')\left(\frac{100}{\pi\psi}\right)$$

When the respective values of y' , y'' , and somal diameter, ψ , are substituted into equation (13) for each of the 104 neurons and values for \hat{y} are plotted against y , the coefficient of determination (r^2) was 0.84 (Figure 6A). If linear equations (3) and (5) are substituted for y' and y'' , then

$$(14) \quad \hat{y} = (1.32 + 0.02\psi)(-27.17 + 2.04\psi)\left(\frac{100}{\pi\psi}\right)$$

In this case, r^2 was 0.76 for \hat{y} plotted against y (Figure 6B). There is even less of a correlation (Figure 6C) between \hat{y} and y ($r^2 = 0.62$) when the curvilinear equations (4) and (6) are used as shown in equation (15).

$$(15) \quad \hat{y} = (0.69\psi^{0.29})(4.312 \times 10^{-3}\psi^{2.56})\left(\frac{100}{\pi\psi}\right)$$

Thus, the equations derived from simple correlation analysis do not predict the percentage of the surface of a motor neuronal profile that is covered by boutons as well as does using the actual measured values for the length and number of boutons. It is clear, too, that equations (13)–(15) predict a coverage by axosomatic boutons that exceeds 100% for many motor neurons.

Another approach, using multiple linear and curvilinear correlation analysis, enabled a more complete test of how well the size and number of boutons and motor neuronal diameter can be used to predict the percentage of the perimeter of a motor neuronal profile that is covered by boutons. Multiple correlation analysis also offers a

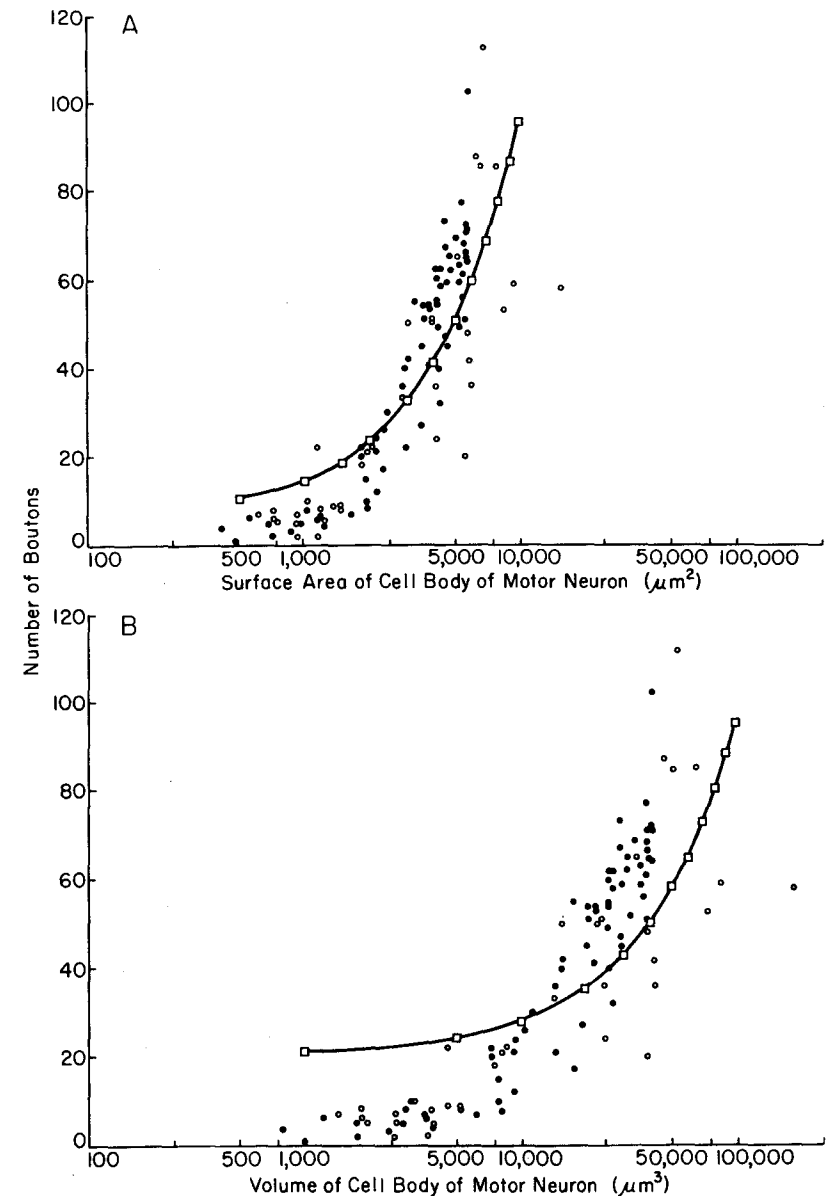


Fig. 5. Number of axosomatic boutons on neurons of different somal surface area (A) and volume (B). Surface area and volume were calculated using equations (8) and (7), respectively. Because the scatter diagrams are plotted on a semilogarithmic scale, the linear estimations (\square) do not appear as a straight line. The fit of the line to the data points is better for surface area than for volume.

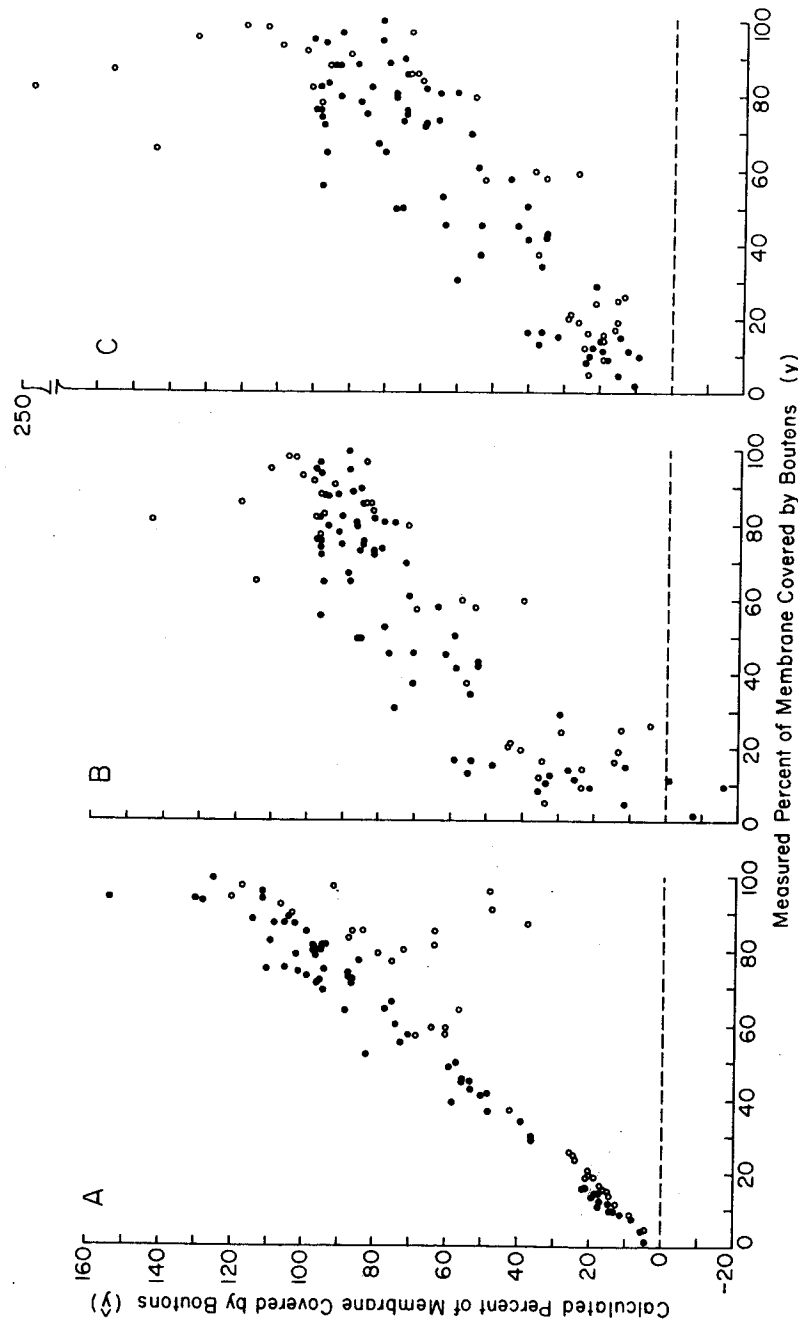


Fig. 6. Correlation between calculated and measured percent of membrane covered by axosomatic boutons. \hat{y} , the amount of coverage predicted for each neuron, is plotted against y , the measured amount of coverage. \hat{y} was calculated using equation (13) for A, (14) for B and (15) for C.

way to look for significant interactions among variables. The multiple linear correlation given by equation (16) has six terms to predict the expected percentage of coverage by boutons (\hat{y}) for each motor neuron.

$$(16) \quad \hat{y} = 35.88 - 2.774\psi - 25.17y' + 2.095y'' + 2.058\psi y' - 0.01785\psi y' y''$$

Figure 7A shows the predicted value (\hat{y}) using equation (16) plotted against the measured value (y) for percent of coverage by boutons on each of the neurons. The coefficient of multiple determination (R^2) was 0.91. Equation (16) suggests significant interactions between the independent variables: motor neuronal diameter, size of boutons and number of boutons (i.e. $\psi \cdot y'$ and $\psi \cdot y' \cdot y''$). The multiple curvilinear correlation given by equation (17) was obtained by first finding the simple terms that seemed most significant using 'stepwise' and 'maximal R' procedures and then by assessing which of the 36 possible interactive terms were significant using a 'stepwise' procedure.

$$(17) \quad \hat{y} = (e^{4.808})(e^{0.4955\psi})(e^{1.167y'})(e^{0.03662y''})(\psi^{-4.725})(y'^{5.792}) \dots \\ \dots (e^{-0.002235\psi^2})(e^{-0.0001455y'^2})(e^{-1.709\ln\psi \ln y''}) \dots \\ \dots (y'^{0.04213\psi})$$

Figure 7B shows a plot of predicted (\hat{y}) versus measured (y) values of the coverage by boutons for each of the motor neurons, where \hat{y} was calculated from equation (17). The coefficient of multiple determination (R^2) was 0.97. Equation (17), also, suggests significant interactions between the independent variables: motor neuronal diameter, size of boutons and number of boutons (i.e. $\ln\psi \cdot \ln y''$ and $\psi \cdot \ln y''$).

Density of Axosomatic Boutons

The density of boutons (DB) is a frequently used measure of the amount of synaptic input to motor neurons (Gelfan and Rapisarda, 1964; Conradi, 1969; Henneman, 1974; Sterling, 1977; Spencer and Sterling, 1977; Limwongse and DeSantis, 1980; Spencer *et al.*, 1980). We use the phrase 'density of boutons' as equivalent to the terms 'synaptic density' and 'packing density' used by other investigators (Gelfan and Rapisarda, 1964; Conradi and Ronnevi, 1975). It is the number of boutons per $100 \mu\text{m}^2$ of postsynaptic surface of the motor neuron. That is different from the density of boutons measured per unit area of neuropil or per unit length of postsynaptic membrane, both of which appear in the literature. As we use the phrase here, density of boutons is not directly measured from a single profile of a sectioned cell seen with the electron microscope; it is calculated from unidimensional measures. At least three methods have been used to do this for motor neurons.

In the one given by Gelfan and Rapisarda (1964), and frequently used by others in studies of motor neurons (Sterling, 1977; Spencer and Sterling, 1977; Limwongse and DeSantis, 1980; Spencer *et al.*, 1980), the number of boutons is the important measure. The average number of boutons per ten linear microns of postsynaptic membrane is squared, so that, where C is the circumference of the neuronal profile,

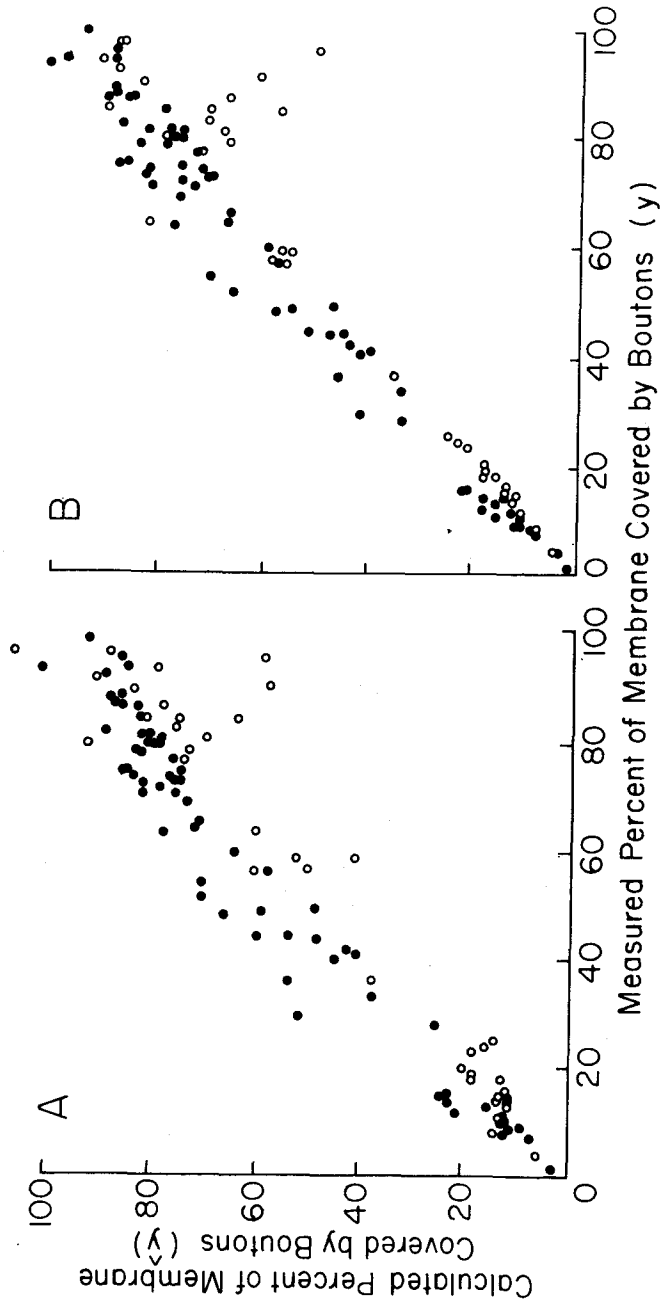


Fig. 7. Accounting for the percent of membrane covered by axosomatic boutons on neurons of different somal diameter using multiple correlation analysis. \hat{y} , the amount of coverage predicted for each neuron is plotted against y , the measured amount of coverage. \hat{y} was calculated using equation (16) obtained by multiple linear correlation (A) and using equation (17) obtained by multiple curvilinear correlation (B).

$$(18) \quad DB_1 = \left[\frac{10y''}{\frac{C}{10\mu m}} \right]^2$$

Conradi and Ronnevi (1975) calculated the density of boutons on motor neurons as the percentage of the neuronal profile covered by boutons (y) divided by the mean area of apposition of the terminals, which was determined on the basis of the average bouton length (y'), so that

$$(19) \quad DB_2 = \frac{y}{4y'^2} = \frac{y\pi}{4y'^2}$$

This method has also been used to calculate the density of boutons on cerebral cortical (Kaiserman-Abramov and Peters, 1972) and Mauthner (Jacoby and Kimmel, 1982) neurons. The third method, proposed by Koziol and Tuckwell (1978), gives the number of boutons per unit area by taking the reciprocal of the square of the average spacing between nearest neighbor boutons (k)

$$(20) \quad DB_3 = \frac{1}{k^2}$$

k^2 may be obtained from linear measures by dividing the average length of boutons (y') apposing the somal profile by the average number of boutons (y'') per unit length of somal circumference (C) so that

$$(21) \quad DB_3 = \frac{1}{y'/(y''/C)} = \frac{y''}{Cy'}$$

We converted values for DB_3 in equation (21) to units equivalent to those for equations (18) and (19) (i.e. number of boutons/100 μm^2) as follows

$$(22) \quad DB_3 = \frac{100y''}{100Cy'}$$

Figure 8 shows scatter diagrams for the density of axosomatic boutons [equations (18), (19) and (22)] plotted against motor neuronal diameter. Equation (18) resulted in a better linear correlation ($r^2 = 0.55$) than did equations (19) and (22), the other two methods for calculating density of boutons (Table 1). However with each of the three methods, the data points were fit best (Table 1) by a power curve. Equation (18) (Figure 8A) again resulted in the highest coefficient of determination ($r^2 = 0.69$). Because values for the exponent in the power curve were close to 1.00 when using equation (19) (Figure 8B) and equation (22) (Figure 8C), those power curves more nearly approximated the straight lines. The notable differences in the curvilinear regressions shown in Figure 8 occurred because of the different measures used and operations performed on them [compare equations (18), (19) and (22)].

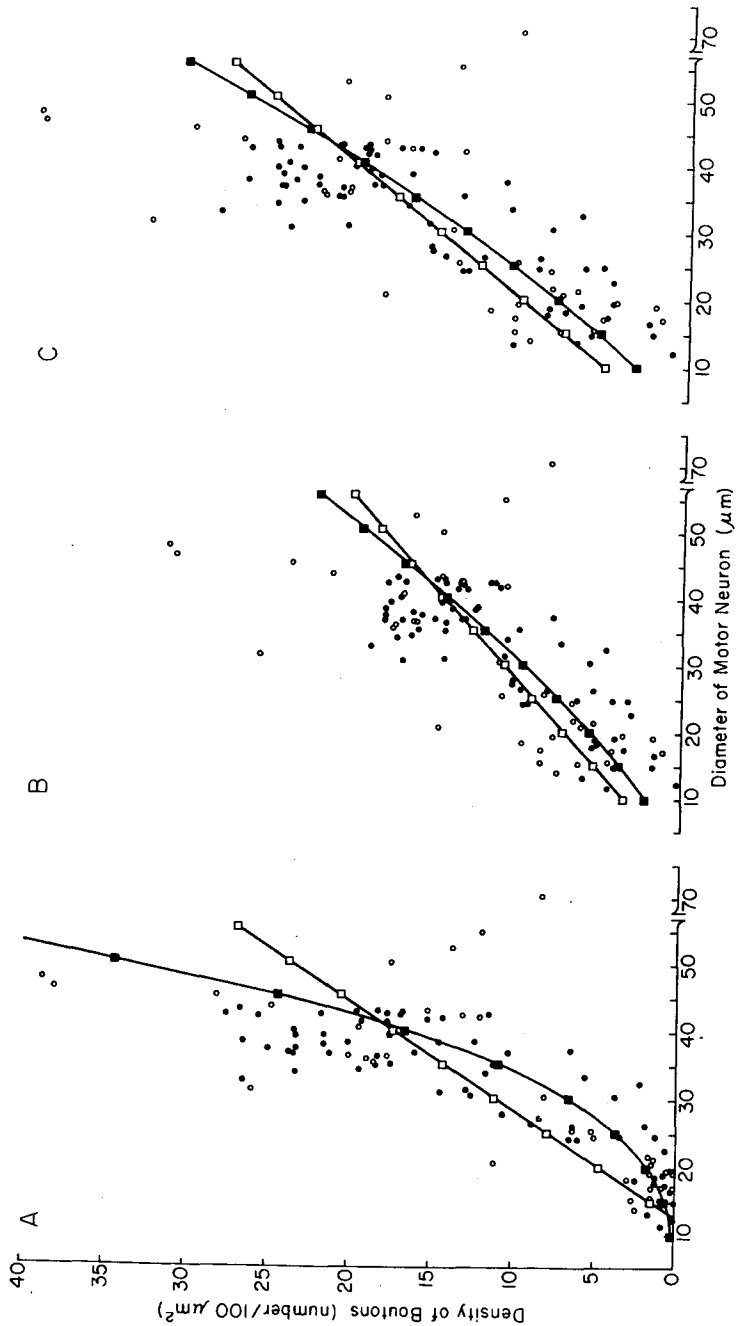


Fig. 8. Density of axosomatic boutons on neurons of different diameter. Values for density of boutons were calculated using equations 18 (A), 19 (B) and 22 (C). Each scatter diagram is fit by a linear equation (\square) and a power curve (\blacksquare). The constants a and b for the linear equations are, respectively: for A (-8.11 , 0.64), for B (-0.23 , 0.38) and for C (0.03 , 0.51). For the power curves, the constants a and b are, respectively: for A (1.224×10^{-4} , 3.20), for B (0.09 , 1.37) and for C (0.15 , 1.33).

When each of the methods for calculating density of boutons was used and the values plotted against estimates of the motor neuron's surface area and volume, coefficients of determination were low (Table 2). But as was the case for the number of boutons, surface area was a better predictor of density of boutons than was the volume of a motor neuron.

4. Discussion

Role of Somatic Surface Area and Volume

Within some populations of vertebrate neurons that have similar morphology except for size, the percentage of the somal surface covered by boutons is positively correlated with the size of the postsynaptic neuron (Bowsher and Westman, 1971; Westman, 1971a,b; Westman and Bowsher, 1971; Newman, 1974; Nakamura, 1975). This condition applied also to neurons which innervated skeletal muscles of the limbs and jaw. For these neurons, greater coverage of the soma was due chiefly to a greater number rather than a greater size of boutons on larger motor neurons as compared to smaller ones. The range in the number of axosomatic boutons had a lower limit that was predicted by the surface area of the motor neuron's soma and an upper limit correlated to the volume of the soma. It is interesting that Lee *et al.* (1982) noted a statistically significant increase in the number of synapses per unit length of postsynaptic membrane on cell bodies of granule cells surviving in the dentate gyrus after X-irradiation was used to reduce the granule cell population. Although quantitative comparisons were not given, the somas of surviving neurons appeared to be larger in size than granule cells in control rats; the average length of axosomatic synapses was not different between groups. Their observations reflect what we would expect if the number of axosomatic boutons increases as a power function of the postsynaptic somal size.

Although analysis by correlation (and regression) provides a method for exploring the ways in which elements are related, it neither assesses causality nor explains phenomena (Ezekiel and Fox, 1959; Sokal and Rohlf, 1969; Huntsberger and Billingsley, 1981). Understanding must be sought in terms of the biology of neural elements, and at least three features of the postsynaptic cell could account for our findings. Sheer physical size of the target cell's somal surface could be important. One might then expect a larger soma to be encountered by axon terminals more frequently than a smaller one (however cf. Jacoby and Kimmel, 1982). Second, electrical potentials and currents associated with the cell membrane may be important determinants. These two explanations relate primarily to the surface of the postsynaptic cell body encountered. A third possibility for why larger motor neurons have more axosomatic boutons is that some substance made in or transported to the cytoplasm of the motor neuron's cell body is responsible for attracting and retaining boutons. The amount of this material might be expected to be present in the motor neuron as the cube of somal diameter, reflecting the volume of the cell body or organelles comprising it.

Role of Retrograde Axonal Transport in the Postsynaptic Neuron

There is evidence that retrograde axonal transport in a neuron does affect the amount of synaptic input it receives. After axotomy of a motor neuron, boutons withdraw from its somatic surface (Blinzinger and Kreutzberg, 1968; Hamberger *et al.* 1970; Torvik and Soreide, 1972; Kerns and Hinsman, 1973; Sumner and Sutherland, 1973; Cull, 1974, 1975a; Chen, 1978). Chemical blockade of axoplasmic transport produces a similar result (Cull 1975b). Axosomatic boutons with clear, round vesicles decrease in preference to those with flattened or pleomorphic vesicles after axotomy (Sumner, 1975). Electrophysiological changes after axotomy include a decrease in the monosynaptic reflex and in the amplitude and synchrony of postsynaptic potentials; spike-like partial depolarizations appear on the excitatory postsynaptic potentials, which have a longer time course (Acheson *et al.*, 1942; Campbell, 1944; Downman *et al.*, 1953; Eccles *et al.*, 1958; McIntyre *et al.*, 1959; Kuno and Llinas, 1970a, b; Mendell *et al.*, 1976). Axonal regeneration and reinnervation of muscle result in a return of synaptic connectivity to the motor neuron (Acheson *et al.*, 1942; Downman *et al.*, 1953; Sumner and Sutherland, 1973; Cull, 1974; Kuno *et al.*, 1974a, b; Sumner, 1976; Goldring *et al.*, 1980). Since axotomy results in swelling of the motor neuron's soma (Brattgård *et al.*, 1957) at about the time axosomatic boutons are being lost, it follows that an increase in cell size alone is not sufficient to account for an increase in the amount of axosomatic input to motor neurons. Similar retrograde changes have been reported for postganglionic autonomic neurons (Brown and Pascoe, 1954; Acheson and Remolina, 1955; Hunt and Riker, 1966; Pilar and Landmesser, 1972; Matthews and Nelson, 1975; Purves, 1975, 1976). The synaptic depression reported for postganglionic sympathetic neurons is partially prevented by exogenous nerve growth factor (Purves and Njå, 1976), a substance selectively taken up and retrogradely transported to the neuronal somata by these neurons (Stockel *et al.*, 1975; Stockel and Thoenen, 1975).

Taking another view, the partial removal of presynaptic input to central and peripheral neurons results in a replacement of boutons onto the postsynaptic neuron by means of collateral sprouting of remaining axons (see reviews by Guth, 1956; Moore, 1974; Puchala and Windle, 1977; Cotman *et al.*, 1981). In the superior cervical ganglion, collateral sprouting of the residual preganglionic axons is accentuated by electrical stimulation of the postganglionic neurons (Maehlen and Njå, 1982).

Together these findings support the notion that the postsynaptic neuron exerts a considerable control over the amount of axosomatic input it normally receives and that retrograde axonal transport may be an important mechanism for this process. The idea that the motor neuron is an important regulator of the axosomatic boutons it receives is consistent with evidence that spinal reflex arcs form in a retrograde direction (Vaughn and Grieshaber, 1973; Sims and Vaughn, 1979) and with a recent study of synapse formation by regenerated retinotectal axons (Murray *et al.*, 1982). However, the postsynaptic cell alone may not completely regulate the amount of synaptic input it normally receives. For example, studies on the development of axodendritic synapses on the Mauthner cell suggest that either the presynaptic neuron

itself (Kimmel *et al.*, 1977) or an interaction between it and the dendrite (Jacoby and Kimmel, 1982) is important. Evidence also exists for an interactive control between pre- and postjunctional cells from studies of the developing neuromuscular junction (O'Brien *et al.*, 1980). There is support from the present study for interaction between the motor neuronal cell body and the boutons that terminate on it since the percentage of the somal membrane covered by boutons was more accurately predicted when interactive terms were included in the multiple correlation equations.

Density of Boutons on Motor Neurons

For motor neurons that innervate limb muscles, there is an inverse relationship between physiological excitability and the size of the cell body (Henneman, 1957; Henneman *et al.*, 1965a, b; Somjen *et al.*, 1965); this has been called the 'size principle' (Henneman *et al.*, 1965a; Burke, 1973). Most of the basic findings have been confirmed for spinal cord motor neurons (Dum and Kennedy, 1980; Fleshman *et al.*, 1981a,b) and extended to trigeminal motor neurons innervating the jaw closer muscles (Desmedt and Godaux, 1975; Goldberg and Derfler, 1977; Clark *et al.*, 1978; Lund *et al.*, 1979) and to motor neurons in invertebrates (Davis, 1971; Kovac *et al.*, 1982). At least two explanations have been proposed to account for the size principle. Originally, the causal factor was considered to be the variation in the amount of input resistance offered by motor neurons of different size (Henneman *et al.*, 1965a,b). More recently, the basis has been explained in terms of the number of branch points and corresponding incidences of transmission failures that occur on afferent fibers as they become presynaptic to the motor neuron (Lüscher *et al.*, 1979, 1983). A fundamental assertion in both explanations has been that the synaptic density is equal on motor neurons of different size (Mendel and Henneman, 1971; Henneman, 1974; Lüscher *et al.*, 1979). The morphological basis for this claim is a light microscopic study done on ventral horn neurons in which the density of boutons was estimated (Gelfan and Rapisarda, 1964). Later studies of ventral horn neurons with the electron microscope have shown that the number of axosomatic boutons (Bodian, 1964) and active zones (synapses) (McLaughlin, 1972), and the percent of the surface of the cell body covered by boutons (Kojima *et al.*, 1972) varies directly with the size of the postsynaptic neuronal soma. The morphological types of axosomatic boutons are also of different proportion for large and small neurons of the ventral horn (Bernstein and Bernstein, 1976). But in these electron microscopic studies, the density of boutons was not evaluated.

We have shown here that the calculated density of axosomatic boutons on trigeminal motor neurons and ventral horn neurons of different size is a direct, curvilinear function of a motor neuron's diameter. This rules out the morphological possibility that axosomatic boutons are distributed in equal density on motor neurons of different size or in a greater density on smaller motor neurons. The finding supports, but does not prove, the argument that the basis for the size principle may be the greater branching of presynaptic fibers with a consequent transmission failure (however cf. Zengel *et al.*, 1983). If all homonymous motor neurons in a pool receive

presynaptic input in proportion to their size (Mendell and Henneman, 1971; Henneman, 1974), and if the total (somatic plus dendritic) bouton density is greater on larger motor neurons, one would expect there to be a greater number of branch points along a fiber's course to a larger motor neuron. Transmission failure at branch points is more likely with spike trains than with single volleys (Scott, 1977), and EPSP amplitude in alpha motor neurons is often depressed when Ia fibers are stimulated at high frequency (Honig *et al.*, 1983).

There are several ways in which the relationships between density of boutons and the size principle may be further clarified. Quantitative data about axodendritic boutons are needed for a large sample of motor neurons of different size. Even if not as strategically placed as axosomatic boutons, the amount of synaptic input to dendrites of motor neurons is thought to exceed that to the soma (see Conradi, 1976, for review). Second, a more direct method of determining the density of boutons is required. Technical methods for doing that are available. Finally, diversity should be explored. For the extraocular system physiological findings are in accord with the size principle (Barmack, 1977), but density of axosomatic boutons is not obviously related to the size of the motor neuron (Sterling, 1977; Spencer and Sterling, 1977; Spencer *et al.*, 1980). There are distinct differences between the extraocular muscles and those of the limbs and jaw in mammals. Extraocular muscles have no bony insertion, little variability in load, very quick twitch durations, two distinct patterns of innervation to muscle fibers, and usually lack muscle spindles; their motor neurons are capable of very high discharge rates, lack a monosynaptic proprioceptive feedback, and receive direct vestibular, internuclear, reticular and cerebellar synaptic input (Carpenter, 1977). Further studies of this system and others which may be like it should provide a more thorough understanding of important variables which underlie motor system function at the level of the motor neuron.

Acknowledgements

We gratefully acknowledge contributions by the following people: illustrations — G. DeSantis, review — Dr. T. McKean and P. Peterson, statistics — Dr. D. Everson and J. Steverson, typing — M. Parrish and J. Schenk. This work was financed in part by U.S.P.H.S. grants NS-11026, RR-05360 and RR-07170. V.L. was supported by the Government of Thailand.

References

- Archeson, G. H., Lee, E. S. and Morison, R. S. (1942). A deficiency in the phrenic respiratory discharges parallel to retrograde degeneration. *J. Neurophysiol.* **5**, 269–273.
- Acheson, G. H. and Remolina, J. (1955). The temporal course of the effects of postganglionic axotomy on the inferior mesenteric ganglion of the cat. *J. Physiol.* **127**, 603–616.
- Barmack, N. H. (1977). Recruitment and suprathreshold frequency modulation of single extraocular muscle fibers in the rabbit. *J. Neurophysiol.* **40**, 779–790.
- Bernstein, J. J. and Bernstein, M. E. (1976). Ventral horn synaptology in the rat. *J. Neurocytol.* **5**, 109–123.

- Blinzinger, K. and Kreutzberg, G. (1968). Displacement of synaptic terminals from regenerating motoneurons by microglial cells. *Zschr. Zellforsch.* **85**, 145–157.
- Bodian, D. (1964). An electron microscopic study of the monkey spinal cord. *Bull. Johns Hopkins Hosp.* **114**, 13–119.
- Bowsher, D. and Westman, J. (1971). Ultrastructural characteristics of the caudal and rostral brain stem reticular formation. *Brain Res.* **28**, 443–457.
- Brattgård, S.-O., Edström, J.-E. and Hydén, H. (1957). The chemical changes in regenerating neurons. *J. Neurochem.* **1**, 316–325.
- Brown, G. L. and Pascoe, J. E. (1954). The effect of degenerative section of ganglionic axons on transmission through the ganglion. *J. Physiol.* **123**, 565–573.
- Burke, R. E. (1973). On the central nervous system control of fast and slow twitch motor units. In: *New Developments in Electromyography and Clinical Neurophysiology*. (Desmedt, J. E., Ed.) vol. 3. pp. 69–94. Karger, Basel.
- Campbell, B. (1944). The effects of retrograde degeneration upon reflex activity of ventral horn neurons. *Anat. Rec.* **88**, 25–37.
- Carpenter, R. H. S. (1977). *Movements of the Eyes*. Pion, London.
- Chen, D. H. (1978). Qualitative and quantitative study of synaptic displacement in chromatolyzed spinal motoneurons of the cat. *J. Comp. Neurol.* **177**, 635–664.
- Clark, R. W., Luschei, E. S. and Hoffman, D. S. (1978). Recruitment order, contractile characteristics, and firing patterns of motor units in the temporalis muscle of monkeys. *Exptl. Neurol.* **61**, 31–52.
- Conradi, S. (1969). Ultrastructure and distribution of neuronal and glial elements on the surface of the proximal part of a motoneuron dendrite, as analyzed by serial sections. *Acta Physiol. Scand., Suppl.* **332**, 49–64.
- Conradi, S. (1976). Functional anatomy of the anterior horn motor neuron. In: *The Peripheral Nerve*. (Landon, D. N., Ed.) pp. 279–329. Chapman and Hall, London.
- Conradi, S. and Ronnevi, L.-O. (1975). Spontaneous elimination of synapses on cat spinal motoneurons after birth: do half of the synapses on the cell bodies disappear? *Brain Res.* **92**, 505–510.
- Cotman, C. W., Nieto-Sampedro, M. and Harris, E. W. (1981). Synapse replacement in the nervous system of adult vertebrates. *Physiol. Rev.* **61**, 684–784.
- Cull, R. E. (1974). Role of nerve-muscle contact in maintaining synaptic connections. *Exptl. Brain Res.* **20**, 307–310.
- Cull, R. E. (1975a). Affect of sensory nerve division on the afferent synapses of axotomized motor neurones. *Exptl. Brain Res.* **22**, 421–425.
- Cull, R. E. (1975b). Role of axonal transport in maintaining central synaptic connections. *Exptl. Brain Res.* **24**, 97–101.
- Davis, W. J. (1971). Functional significance of motoneuron size and soma position in swimmeret system of the lobster. *J. Neurophysiol.* **34**, 274–288.
- Desmedt, J. E. and Godaux, E. (1975). Vibration-induced discharge patterns of single motor units in the masseter muscle in man. *J. Physiol.* **253**, 429–442.
- Downman, C. B. B., Eccles, J. C. and McIntyre, A. K. (1953). Functional changes in chromatolyzed motoneurons. *J. Comp. Neurol.* **97**, 9–36.
- Dum, R. P. and Kennedy, T. T. (1980). Physiological and histochemical characteristics of motor units in cat tibialis anterior and exterior digitorum longus muscles. *J. Neurophysiol.* **43**, 1615–1630.
- Eccles, J. C., Libet, B. and Young, R. R. (1958). The behavior of chromatolyzed motoneurons studied by intracellular recording. *J. Physiol.* **143**, 11–40.
- Ezekiel, M. and Fox, K. A. (1959). *Methods of Correlation and Regression Analysis. Linear and Curvilinear*. 3rd edition. John Wiley and Sons, New York.
- Fleshman, J. W., Munson, J. B. and Sypert, G. W. (1981a). Homonymous projection of individual group Ia-fibers to physiologically characterized medial gastrocnemius motoneurons in the cat. *J. Neurophysiol.* **46**, 1339–1348.

- Fleshman, J. W., Munson, J. B., Sypert, G. W. and Friedman, W. A. (1981b). Rheobase, input resistance, and motor-unit type in medial gastrocnemius motoneurons in the cat. *J. Neurophysiol.* **46**, 1326-1338.
- Gelfan, S. and Rapisarda, A. F. (1964). Synaptic density on spinal neurons of normal dogs and dogs with experimental hind-limb rigidity. *J. Comp. Neurol.* **123**, 73-96.
- Goldberg, L. J. and Derfler, B. (1977). Relationship among recruitment order, spike amplitude, and twitch tension of single motor units in human masseter muscle. *J. Neurophysiol.* **40**, 879-890.
- Goldring, J. M., Kuno, M., Núñez, R. and Snider, W. D. (1980). Reaction of synapses on motoneurons to section and restoration of peripheral sensory connexions in the cat. *J. Physiol.* **309**, 185-198.
- Guth, L. (1956). Regeneration in the mammalian peripheral nervous system. *Physiol. Rev.* **36**, 441-478.
- Hamberger, A., Hansson, H.-A. and Sjöstrand, J. (1970). Surface structure of isolated neurons: detachment of nerve terminals during axon regeneration. *J. Cell Biol.* **47**, 319-331.
- Henneman, E. (1957). Relation between size of neurons and their susceptibility to discharge. *Science* **126**, 1345-1347.
- Henneman, E. (1974). Principles governing distribution of sensory input to motor neurons. In: *The Neurosciences. Third Study Program.* (Schmitt, F. O. and Worden, F. G., Eds.) pp. 281-291. MIT Press, Cambridge.
- Henneman, E., Somjen, G. and Carpenter, D. O. (1965a). Functional significance of cell size in spinal motoneurons. *J. Neurophysiol.* **28**, 560-580.
- Henneman, E., Somjen, G. and Carpenter, D. O. (1965b). Excitability and inhibibility of motoneurons of different sizes. *J. Neurophysiol.* **28**, 599-620.
- Honig, M. G., Collins, W. F. and Mendell, L. M. (1983). α -Motoneuron EPSPs exhibit different frequency sensitivities to single IA-afferent fiber stimulation. *J. Neurophysiol.* **49**, 886-901.
- Hunt, C. C. and Riker, W. K. (1966). Properties of frog sympathetic neurons in normal ganglia and after axon section. *J. Neurophysiol.* **29**, 1096-1114.
- Huntsberger, D. V. and Billingsley, P. (1981). *Elements of Statistical Inference.* 5th edition. Allyn and Bacon, Boston.
- Jacoby, J. and Kimmel, C. B. (1982). Synaptogenesis and its relation to growth of the postsynaptic cell: a quantitative study of the developing Mauthner neuron of the axolotl. *J. Comp. Neurol.* **204**, 364-376.
- Kaiserman-Abramov, I. R. and Peters, A. (1972). Some aspects of the morphology of Betz cells in the cerebral cortex of the cat. *Brain Res.* **43**, 527-546.
- Kerns, J. M. and Hinsman, E. J. (1973). Neuroglial response to sciatic neurectomy. II. Electron microscopy. *J. Comp. Neurol.* **151**, 255-279.
- Kimmel, C. B., Schabtach, E. and Kimmel, R. J. (1977). Developmental interactions in the growth and branching of the lateral dendrite of Mauthner's cell (*Ambystoma mexicanum*). *Dev. Biol.* **55**, 244-259.
- Kojima, T., Saito, K. and Kakimi, S. (1972). Electron microscopic quantitative observations on the neuron and the terminal boutons contacted with it in the ventrolateral part of the anterior horn (C₆₋₇) of the adult cat. *Okajimas Folia Anatomica Japonica* **49**, 175-226.
- Kovac, M. P., Davis, W. J., Matera, E. and Gillette, R. (1982). Functional and structural correlates of cell size in paracerebral neurons of *Pleurobranchaea californica*. *J. Neurophysiol.* **47**, 909-927.
- Koziol, J. A. and Tuckwell, H. C. (1978). Analysis and estimation of synaptic densities and their spatial variation on the motoneuron surface. *Brain Res.* **150**, 617-624.
- Kuno, M. and Llinas, R. (1970a). Enhancement of synaptic transmission by dendritic potentials in chromatolysed motoneurons of the cat. *J. Physiol.* **210**, 807-821.
- Kuno, M. and Llinas, R. (1970b). Alterations of synaptic action in chromatolysed motoneurons of the cat. *J. Physiol.* **210**, 823-838.
- Kuno, M., Miyata, Y. and Muñoz-Martinez, E. J. (1974a). Differential reaction of fast and slow α -motoneurons to axotomy. *J. Physiol.* **240**, 725-739.
- Kuno, M., Miyata, Y. and Muñoz-Martinez, E. J. (1974b). Properties of fast and slow alpha motoneurons following motor reinnervation. *J. Physiol.* **242**, 273-288.
- Lee, K. S., Gerbrandt, L. and Lynch, G. (1982). Axo-somatic synapses in the normal and x-irradiated dentate gyrus: factors affecting the density of afferent innervation. *Brain Res.* **249**, 51-56.
- Limwongse, V. (1980). The ultrastructural morphology of neurons comprising the trigeminal motor nucleus in the rat, including a quantitative study of axosomatic and axodendritic synapses. Dissertation (1979). Georgetown University, Washington. University Microfilms International, Ann Arbor. **40/7**, 2949-B.
- Limwongse, V. and DeSantis, M. (1980). Coverage by axosomatic boutons varies directly with the diameter of the postsynaptic motor neuron in the trigeminal nucleus of the rat. *Brain Res.* **189**, 239-244.
- Lund, J. P., Smith, A. M., Sessle, B. J. and Murakami, T. (1979). Activity of trigeminal α - and γ -motoneurons and muscle afferents during performance of a biting task. *J. Neurophysiol.* **42**, 710-725.
- Lüscher, H.-R., Ruenzel, P. and Henneman, E. (1979). How the size of motoneurons determines their susceptibility to discharge. *Nature* **282**, 859-861.
- Lüscher, H.-R., Ruenzel, P. and Henneman, E. (1983). Composite EPSPs in motoneurons of different sizes before and during PTP; implications for transmission failure and its relief in Ia projections. *J. Neurophysiol.* **49**, 269-289.
- Maehlen, J. and Njå, A. (1982). The effects of electrical stimulation on sprouting after partial denervation of guinea-pig sympathetic ganglion cells. *J. Physiol.* **322**, 151-166.
- Matthews, M. R. and Nelson, V. H. (1975). Detachment of structurally intact nerve endings from chromatolytic neurones of rat superior cervical ganglion during the depression of synaptic transmission induced by postganglionic axotomy. *J. Physiol.* **245**, 91-135.
- McIntyre, A. K., Bradley, R. and Brock, L. G. (1959). Responses of motoneurons undergoing chromatolysis. *J. Gen. Physiol.* **42**, 931-958.
- McLaughlin, B. J. (1972). The fine structure of neurons and synapses in the motor nuclei of the cat spinal cord. *J. Comp. Neurol.* **144**, 429-460.
- Mendell, L. M. and Henneman, E. (1971). Terminals of single Ia fibers: location, density, and distribution within a pool of 300 homonymous motoneurons. *J. Neurophysiol.* **34**, 171-187.
- Mendell, L. M., Munson, J. B. and Scott, J. G. (1976). Alterations of synapses on axotomized motoneurons. *J. Physiol.* **255**, 67-79.
- Moore, R. Y. (1974). Central regeneration and recovery of function: the problem of collateral reinnervation. In: *Plasticity and Recovery of Function in the Central Nervous System.* (Stein, D. G., Rosen, J. J. and Butters, N., Eds.) pp. 111-128. Academic Press, New York.
- Murray, M., Sharma, S. and Edwards, M. A. (1982). Target regulation of synaptic number in the compressed retinotectal projection of goldfish. *J. Comp. Neurol.* **209**, 374-385.
- Nakamura, Y. (1975). An electron microscope study of the red nucleus in the cat, with special reference to the quantitative analysis of the axosomatic synapses. *Brain Res.* **94**, 1-17.
- Newman, D. B. (1976). The morphology and synaptic organization of neurons in the metencephalic reticular formation in turtles of the genera *Pseudemys* and *Chrysemys*. Dissertation, Loyola University, Chicago. University Microfilms International, Ann Arbor. **36/11**, 4391-B.
- O'Brien, R. A. D., Ostberg, A. J. and Vrbová, G. (1980). The effect of acetylcholine on the function and structure of the developing mammalian neuromuscular junction. *Neurosci.* **5**, 1367-1379.
- Pilar, G. and Landmesser, L. (1973). Axotomy mimicked by localized colchicine application. *Science* **177**, 1116-1118.
- Puchala, E. and Windle, W. F. (1977). The possibility of structural and functional restitution after spinal cord injury. A review. *Exptl. Neurol.* **55**, 1-42.
- Purves, D. (1975). Functional and structural changes in mammalian sympathetic neurones following interruption of their axons. *J. Physiol.* **252**, 429-463.
- Purves, D. (1976). Functional and structural changes in mammalian sympathetic neurones following colchicine application to post-ganglionic nerves. *J. Physiol.* **259**, 159-175.

- Purves, D. and Njå, A. (1976). Effect of nerve growth factor on synaptic depression after axotomy. *Nature* **260**, 535-536.
- Rall, W. (1967). Distinguishing theoretical synaptic potentials computed for different somadendritic distributions of synaptic input. *J. Neurophysiol.* **30**, 1138-1168.
- Sato, M., Mizuno, N. and Konishi, A. (1977). Postnatal differentiation of cell body volumes of spinal motoneurons innervating slow-twitch and fast-twitch muscles. *J. Comp. Neurol.* **175**, 27-36.
- Schadé, J. P. and Van Harreveld, A. (1961). Volume distribution of moto- and interneurons in the peroneus-tibialis neuron pool of the cat. *J. Comp. Neurol.* **117**, 387-398.
- Scott, A. C. (1977). *Neurophysics*. John Wiley, New York.
- Sims, T. J. and Vaughn, J. E. (1979). The generation of neurons involved in an early reflex pathway of embryonic mouse spinal cord. *J. Comp. Neurol.* **183**, 707-720.
- Sokal, R. R. and Rohlf, F. J. (1969). *Biometry*. W. H. Freeman, San Francisco.
- Somjen, G., Carpenter, D. O. and Henneman, E. (1965). Responses of motoneurons of different sizes to graded stimulation of supraspinal centers of the brain. *J. Neurophysiol.* **28**, 958-965.
- Spencer, R. F., Baker, R. and McCrea, R. A. (1980). Localization and morphology of cat retractor bulbi motoneurons. *J. Neurophysiol.* **43**, 754-770.
- Spencer, R. F. and Sterling, P. (1977). An electron microscope study of motoneurons and interneurons in the cat abducens nucleus identified by retrograde intraaxonal transport of horseradish peroxidase. *J. Comp. Neurol.* **176**, 65-86.
- Sterling, P. (1977). Anatomy and physiology of goldfish oculomotor system. I. Structure of abducens nucleus. *J. Neurophysiol.* **40**, 557-572.
- Stockel, K., Schwab, M. and Thoenen, H. (1975). Comparison between the retrograde axonal transport of nerve growth factor and tetanus toxin in motor, sensory and adrenergic neurons. *Brain Res.* **99**, 1-16.
- Stockel, K. and Thoenen, H. (1975). Retrograde axonal transport of nerve growth factor: specificity and biological importance. *Brain Res.* **85**, 337-341.
- Sumner, B. E. H. (1975). A quantitative analysis of the response of presynaptic boutons to postsynaptic motor neuron axotomy. *Exptl. Neurol.* **46**, 605-615.
- Sumner, B. E. H. (1976). Quantitative ultrastructural observations on the inhibited recovery of the hypoglossal nucleus from the axotomy response when regeneration of the hypoglossal nerve is prevented. *Exptl. Brain Res.* **26**, 141-150.
- Sumner, B. E. H. and Sutherland, F. I. (1973). Quantitative electron microscopy on the injured hypoglossal nucleus in the rat. *J. Neurocytol.* **2**, 315-328.
- Torvik, A. and Soreide, A. J. (1972). Nerve cell regeneration after axon lesions in newborn rabbits. A light and electron microscopic study. *J. Neuropathol. Exptl. Neurol.* **31**, 683-695.
- Ulfhake, B. and Cullheim, S. (1981). A quantitative light microscopic study of the dendrites of cat spinal γ -motoneurons after intracellular staining with horseradish peroxidase. *J. Comp. Neurol.* **202**, 585-596.
- Vaughn, J. A. and Grieshaber (1973). A morphological investigation of an early reflex pathway in developing rat spinal cord. *J. Comp. Neurol.* **148**, 177-210.
- Voss, Ch., Shiller, A., and Taugner, R. (1980). Morphology and distribution of the synapses to the spinal motoneuron of the frog. *Cell Tiss. Res.* **213**, 253-271.
- Westman, J. (1971a). Quantitative estimation of the proportion of perikaryal surface area covered by boutons — a possibility to distinguish different nerve cell populations. *Brain Res.* **32**, 203-207.
- Westman, J. (1971b). The lateral cervical nucleus in the cat. V. A quantitative evaluation on the bouton- and glia- covered surface area of different LCN neurons. *Zschr. Zellforsch.* **115**, 377-387.
- Westman, J. and Bowsher, D. (1971). The fine structure of "non-specific" grey matter (laminae V and VII) in the cat spinal cord. *Exptl. Brain Res.* **12**, 379-388.
- Zengel, J. E., Reid, S. A., Sypert, G. W. and Munson, J. B. (1983). Presynaptic inhibition, EPSP amplitude, and motor-unit type in triceps surae motoneurons in the cat. *J. Neurophysiol.* **49**, 922-931.